PERGAMON

Vacuum 64 (2002) 15–31

VACUUM
SURFACE ENGINEERING, SURFACE INSTRUMENTATION & VACUUM TECHNOLOGY

www.elsevier.com/locate/vacuum

Vacuum problems of miniaturization of vacuum electronic components: a new generation of compact photomultipliers ☆

B. Erjavec*

Institute of Metals and Technology, Lepi pot 11, 1000 Ljubljana, Slovenia

Received 14 March 2001; accepted 30 March 2001

Abstract

Recently, a new generation of compact photomultipliers exhibiting high sensitivity, fast time response, extremely low background and extended dynamic range has been introduced. The electron multiplication is enabled by a high-gain and extremely low-background, closed-end, channel electron multiplier serving also as a body of the new mini electron tube. By preventing ultra-fine leaks by the introduction of ultra-sensitive leak detection, and incorporating a high performance getter material, the new channel photomultiplier becomes a very small volume static vacuum system with a relatively large inner surface, evolving gases with different outgassing rates. For an extended channel photomultiplier lifetime, it is of great importance to maintain extreme vacuum conditions and therefore the tube bodies have to be pre-conditioned by a thorough UHV baking followed by an effective electron and UV light scrubbing. Semitransparent photocathodes are remotely processed, onto many faceplates in one cycle, in order to maximize quantum efficiency at the chosen wavelength, minimize photocathode dark current and ensure excellent uniformity. The faceplates are hermetically sealed to the tube bodies during the course of a vacuum transfer technique. The tube shelf life is mainly dependent on the photocathode stability in an alkali-free environment inside the tube while the tube operational life is dependent on the intensity of ion bombardment of the photocathode reflecting both in the ejection of secondary electrons followed by the formation of spurious pulses and photocathode surface sputtering. Possible sources of chemically inert gases, which can affect the correct functioning of the tubes are discussed. © 2001 Elsevier Science Ltd. All rights reserved.

Keywords: Ultra-fine leaks; Getter sorption capacity; Ambient temperature outgassing; Electron stimulated outgassing; He permeation; Photocathode stability; Pulse height distribution; After-pulses

1. Introduction

For applications in biotechnology, life science and analytical instrumentation, in the investigation of biological, medical and chemical probes and in basic research, there is a need for very sensitive and low background photodetectors. In many cases detection of single photons is required. Seven decades after the invention of the photomultiplier, a new generation of compact photodetectors has been developed, which use the unique characteristics of a photomultiplier, but which also show additional important advantages

☆ Invited talk, presented at JVC-8, June 2000, Pula, Croatia.

*Corresponding author. Tel.: +386-1-470-1835; fax: +386-1-470-1939.

E-mail addresses: bojan.erjavec@imt.si (B. Erjavec).

0042-207X/01/$ - see front matter © 2001 Elsevier Science Ltd. All rights reserved.
PII: S0042-207X(01)00366-9

[1–3]. In comparison with conventional photomultipliers the anode sensitivity of the new photosensor is strongly increased while, simultaneously, the tube background current is extremely reduced. The sensor is easy to use and is more rugged than conventional photomultipliers. The design is compact, smart, and simple to integrate. No external voltage divider network is required.

1.1. Principle of operation of a new channel photomultiplier

Fig. 1 shows a schematic cross-section of a new channel photomultiplier (CPM) with main tube components, and a potential distribution during operation in analogue and photon counting mode, respectively. The CPM consists of two main parts: a tube body and a cathode sub-assembly. The hermetically tight tube body consists of a glass insulation ring, a channel electron multiplier (CEM) and an anode sub-assembly. The cathode sub-assembly contains a photocathode faceplate and a metal ring with a spot-welded getter strip. The CPM is assembled in UHV during the course of a vacuum transfer technique.

As for the conventional head-on photomultiplier tube (PMT) light illuminates a semiconductive and semi-transparent photocathode, which is deposited on the entrance window. Due to the external photoeffect light is absorbed inside the photocathode layer and converted into photoelectrons, which are emitted into the vacuum. The photoelectrons are accelerated towards the anode by a high electrical field. On the way to the anode they have to pass through a thin and curved channel. Each time electrons hit the wall of the channel, secondary electrons are ejected out of a very thin surface emissive layer. These secondary electrons accelerate down the channel, hit the channel wall and create still more secondary electrons. This process is repeated several times. Ultimately, an avalanche effect with an electron gain exceeding 10^8 can be obtained. The resulting current can be read out at the anode. The curved shape of the channel provides a defined electron multiplication effect and prevents ion feedback.

This principle of electron multiplication has been used for many years in CEMs operating in a vacuum as independent units. The CEMs are able to detect single electrons, ions, vacuum UV photons and soft X-rays [4]. As shown in Fig. 1 the channel serves as an enclosure for the new electron tube, which is hermetically closed at the back end by the anode sub-assembly using a glass solder. The sealing of the entrance window, with a deposited photocathode layer, to the channel front end is performed in UHV using a metal solder. The applied solder has good wettability on metallized glass surfaces and good low temperature malleability, therefore, it compensates for some differences in the coefficient of expansion when dissimilar materials are to be soldered.

The electron tube is encapsulated inside a plastic housing and held with a silicon rubber potting material. The potting has some important advantages for the CPM operation: First, electrical high voltage immunity is provided, second, the potting

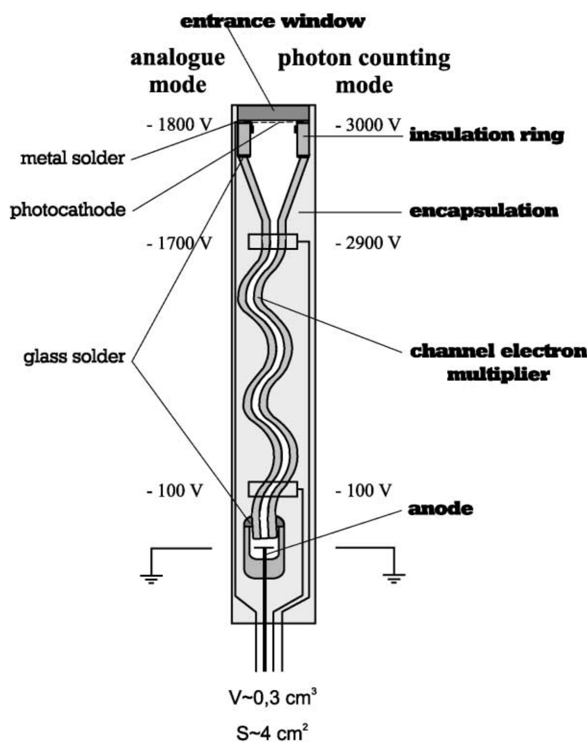

Fig. 1. Cross-section of encapsulated channel electron photomultiplier (CPM) with main components and potential distribution during operation in analogue and photon counting mode.

material secures thermal stability of the CEM and third, it guarantees a good mechanical stability even for strong impacts.

To guarantee the delivery of secondary electrons for sustaining the electron multiplication process, taking place in a very thin surface emissive layer consisted mainly of SiO_2, the channel walls are coated with a thin surface conductive underlayer. The base material of the channel is a proprietary lead silicate glass. During the firing under hydrogen atmosphere the lead oxide is partly reduced and the channel near the surface layer becomes conductive. Applying a high voltage between the channel entrance and exit, a bias current flows through this layer. Since the potting material is in direct thermal contact with the channel glass, Joule-heat developed from the bias current is conducted away from the channel. Compared to the open CEMs operating inside vacuum surroundings, this technique allows a 3–30 times higher bias current, leading to higher maximum linear anode currents as well as higher maximum count rates and extends the dynamic range of the device.

Different input windows made from kovar, UV and quartz glass as well as from crystals like MgF_2 can be sealed to the tube body. Therefore, photocathode spectral sensitivity extending into the vacuum-UV range (115 nm) can be guaranteed, since the lower limit of the spectral range is defined by the choice of the window material. The upper limit of the spectral range or photoelectric threshold wavelength is defined by the choice of the photocathode, therefore many different photocathode materials are deposited by vacuum evaporation, such as alkali iodides, alkali tellurides and alkali antimonides, with maximum photoresponse in the vacuum UV, UV and visible range of the light spectrum, respectively. The photocathode spectral sensitivity of one version of multialkali antimonide photocathodes extends deep into the near IR range (over 900 nm) [5].

1.2. CPM lifetime

The CPM shown in Fig. 1 is very compact. The tube diameter, including encapsulation, is 10.5 mm and its length is 75 mm. The entrance window has a diameter of 9 mm and the diameter of the photocathodes equals 6 mm. The volume of the mini electron tube is about 0.3 cm^3 only, so the CPM represents one of the smallest electron tubes ever produced. In comparison, the volume of conventional PMTs is typically several tens to hundreds cm^3. The inner surface area of the new CPM is about 4 cm^2, therefore a thorough vacuum treatment of the CPM components is necessary because even a small gas evolution may lead to a distinct pressure rise inside the tube. When designing the CPM components care has to be taken in selecting UHV compatible materials. Special UHV cleaning procedures have been developed to remove residuals before inserting the components into a vacuum chamber. A high performance getter material has been introduced assuring a long lifetime.

Due to the small volume of CPM its shelf life and operational life depend mainly on the quality of vacuum after the tube processing; that means on the amount and composition of residual gases inside the tube, during storage and operation, respectively. A schematic cross-section of an unpotted CPM with potential external and internal gas sources is shown in Fig. 2. The first internal gas source is metal solder outgassing while sealing the entrance window, with a deposited photocathode layer, to the tube body. The next internal gas source is ambient temperature outgassing of the tube inner surface taking place during the CPM storage. Possible external gas sources are ultra-fine leaks due to the porosity of an In alloy seal and glass frit seals. Permeation of He, mainly through a quartz input window and, to a lesser extent through glass walls of the tube body and other glass input windows, is an unavoidable external gas source. Two very important internal gas sources during the CPM operation are electron stimulated outgassing from a thin channel surface layer accompanying the electron multiplication process, and photon stimulated outgassing from a thicker cone surface layer due to illumination with transmitted UV light.

Due to the CPM compactness, the preparation of sub-assemblies and the technology of processing have to be optimized very carefully in every detail. If not, the excess gas load cannot be compensated

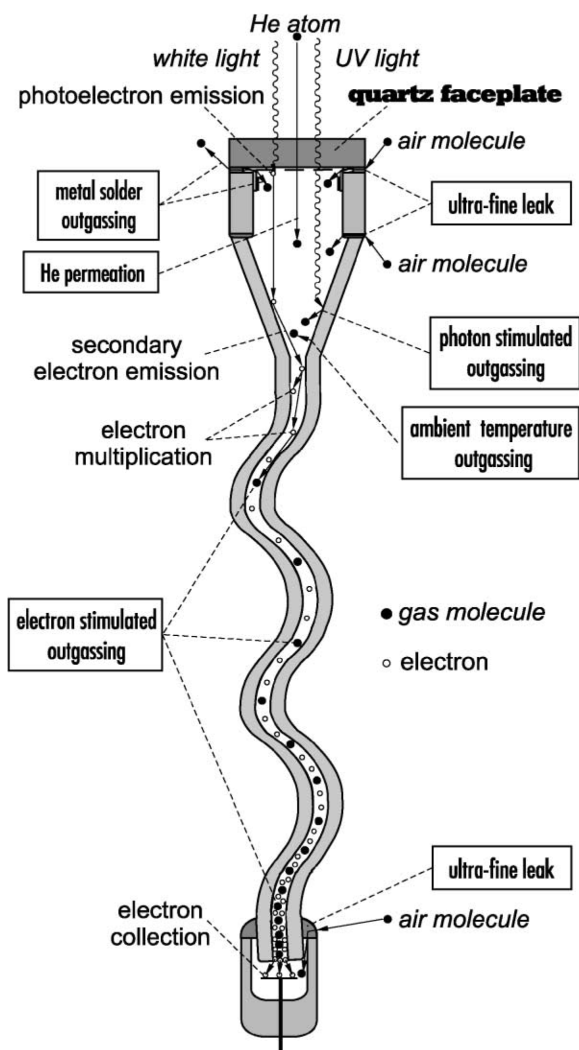

Fig. 2. Cross-section of unpotted CPM with potential external and internal gas sources.

by the available sorption capacity of incorporated (and for safety overdimensioned) getter material. The increased pressure can strongly affect the CPM lifetime. In Fig. 3, a CPM lifetime 'flow-chart' is presented. The CPM lifetime or the stability of anode sensitivity depends on the stability of photocathode sensitivity during CPM storage and operation, and the stability of electron gain during CPM operation. The stability of photocathode sensitivity during the storage depends on the residual alkali vapour pressure prevailing inside the tube. Electron gain decay during the operation is a consequence of either insufficient electron scrubbing, which means that the CEM was not scrubbed to its gain plateau during the CPM processing, or consumed total output charge, when the gain cannot be maintained any further by increasing the applied voltage without increasing the CEM background [4]. The decrease in photocathode sensitivity or quantum efficiency (QE) decay due to chemical reactions of the photocathode layer with residual gases (during storage) and photocathode surface etching by ion bombardment (during operation) are a consequence of the excess gas load, resulting from the different gas sources described above.

1.3. Steps taken to solve vacuum problems

The first requirement to extend the CPM lifetime is an extremely vacuum tight tube envelope. Therefore, we have been paying special attention to the sealing techniques, which are used in the CPM construction. Glass soldering which takes place under the protective atmosphere of N_2 is used to complete the tube body. Metal soldering which has to be performed in UHV is used to seal a cathode sub-assembly to the tube body. To check these two sealing techniques for ultra-fine leaks, which cannot be detected by a commercial dry He-leak detector, we have started to use the ultra-sensitive leak detection based on the rate of pressure rise method.

The metal soldering in UHV is a part of a vacuum transfer technique, which has been developed for CPM batch processing. Besides high volume production this technique enables separate conditioning of the CPM sub-assemblies, which consists of UHV baking of the CPM sub-assemblies, mechanical stirring of the molten In alloy and electron (UV light) scrubbing of the tube bodies. Using a reliable Bayard-Alpert gauge (BAG) and a sensitive residual gas analyser (RGA) we have introduced continuous monitoring of the residual atmosphere during the course of each phase, in order to reduce the outgassing of the CPM components during storage and operation to a minimum.

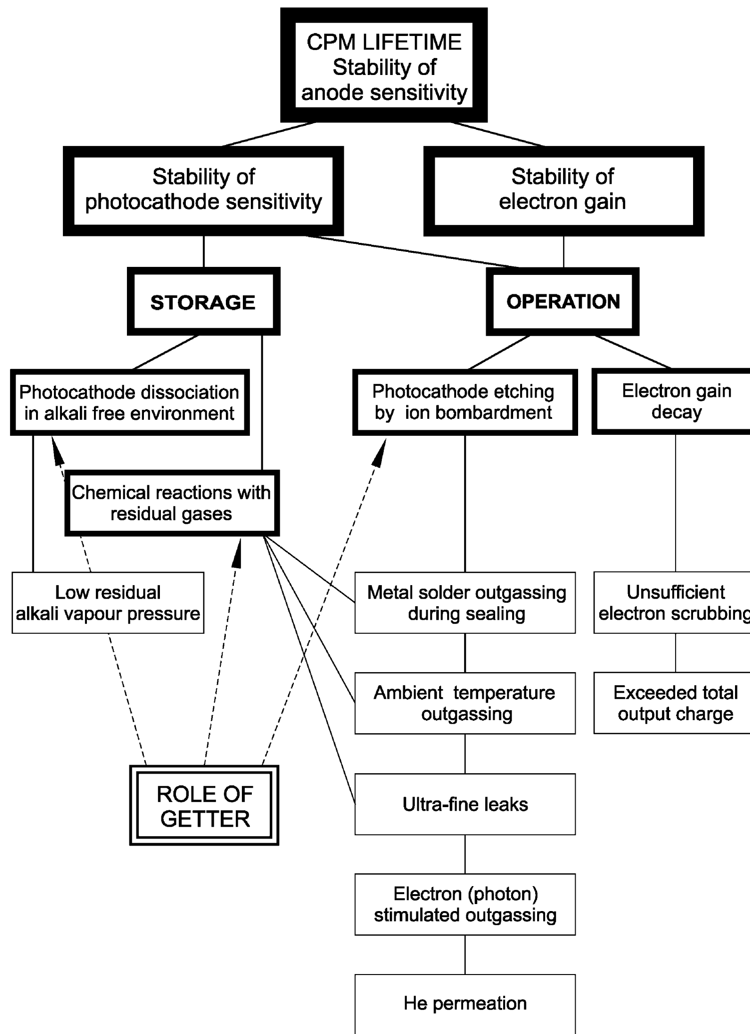

Fig. 3. CPM lifetime 'flow chart'.

Special attention has also been paid to the selection and dimensioning of the getter material. Due to the compact design of CPM, the use of a highly effective non-evaporable getter with a low activation temperature is the only possibility. In this case, the getter activation can be accomplished during the course of the vacuum transfer technique. The continuous monitoring of the residual atmosphere composition while conditioning the tube subassemblies is very important for the CPM lifetime. Although H_2 and CO evolving during the CPM operation are effectively sorbed by the incorporated getter, one must bear in mind that chemically inert gases such as He, Ne and Ar as well as CH_4 (at RT) are not sorbed at all.

2. Experimental

2.1. External gases and CPM subassembly preparation

As already mentioned, an extremely vacuum tight tube envelope is needed to assure a lengthy

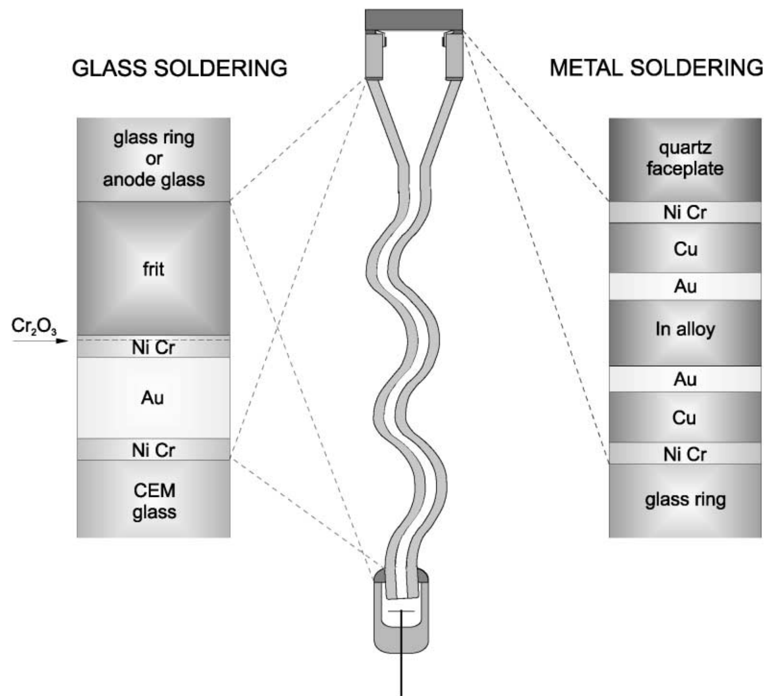

Fig. 4. Cross-section of three CPM main seals: two glass frit seals and an In alloy seal.

CPM lifetime. Both sealing techniques: the glass soldering, which is used to complete the tube body, and the metal soldering, which is used to seal the cathode sub-assembly to the tube body, have been optimized in every detail. A schematic cross-section of three main CPM seals: two glass frit seals and an In alloy seal is presented in Fig. 4. A stable glass frit is used to seal the glass insulation ring and the anode sub-assembly to the metallized channel front and back end, respectively. Metallization layers, consisting of an Au layer with an NiCr underlayer and overlayer are needed to bring electric potentials from external contacts through the seals to the channel entrance and exit. An In alloy is used to seal the metallized photocathode faceplate to a metallized glass insulation ring. Besides bringing electric potential to the photocathode, metallization layers consisting of a Cu layer with an NiCr underlayer and an Au overlayer are needed for the optimum In alloy wetting and vacuum-tight sealing of the glass parts. We have tested two eutectic alloys: In–Sn with a melting point of 117°C and In–Bi with a melting point of 72°C.

2.1.1. *Ultra-fine leaks and ultra-sensitive leak detection*

Possible sources of very small leaks are porous glass frit seals as well as a porous In alloy seal. In order to avoid miniature leaks in the first case, a thin Cr_2O_3 layer is required on top of the metallization layer to establish binding with the glass solder. Although the thin In_2O_3 layer covering the molten In alloy is reduced to gaseous In_2O at temperatures higher than 360°C [6], the excessive oxidation of the In alloy surface is to be prevented, in order to achieve reliable sealing in the second case.

After the glass soldering, vacuum tightness of all tube bodies is tested using a dry He-leak detector. This is used in order to prevent contamination with hydrocarbons and normally has a minimum detectable He leak rate in the low 10^{-10} mbarl/s range. Measurements of vacuum tightness of this

order of magnitude are too rough for small volume electron tubes such as the new CPMs. Leak rates lower than 1×10^{-10} mbarl/s have been defined as ultra-fine leaks. In the case of an ultra-fine leak rate $Q = 1 \times 10^{-12}$ mbarl/s, the corresponding gas load after $\Delta t = 2$ years amounts to $Q\,\Delta t = V\,\Delta P = 6.3 \times 10^{-5}$ mbarl, resulting in a pressure increase $\Delta P \sim 0.2$ mbar in a volume $V \sim 0.3\,\mathrm{cm}^3$. Getterable gases can be sorbed for more than two years if, for instance, a highly efficient non-evaporable getter with a geometric surface area of $0.1\,\mathrm{cm}^2$ and a total sorption capacity of $7 \times 10^{-4}\,\mathrm{mbarl/cm}^2$ is incorporated. Unfortunately, in the case of an air leak containing about 1% of Ar by volume, the partial pressure of Ar is increased to about 2×10^{-3} mbar, therefore the CPM operation is menaced much earlier. On the other hand, photocathodes act as a getter due to their chemical reactivity. The QE behaviour, reflected first in a slight increase and then in a constant decay of multialkali-antimonide photocathodes comprising a thin Cs surface layer, may be an additional indication of ultra-fine leaks in the processed CPMs.

To prevent any ultra-fine leak we have started to perform sample testing of the most critical CPM seals by means of an ultra-sensitive leak detection, which is based on the rate of pressure rise method. Using a spinning rotor gauge (SRG—Viscovac VM212, Leybold) being an inert gauge with a high long-term stability, measurements of a pressure rise ΔP in a known small volume V for a longer time Δt (at constant temperature T) are enabled. From the slope of the linear part of the pressure rise curve, an ultra-fine leak rate is determined as $Q = V\,\Delta P/\Delta t$. For test samples with a volume of the order of $10\,\mathrm{cm}^3$, the sensitivity of the method can be extended into the 10^{-15} mbarl/s range [7]. However, interpreting the measurements of vacuum tightness on test samples constructed from different materials, one should consider contributions due to the outgassing of H_2 from metal parts and the permeation of atmospheric He through the walls of glass parts.

Due to the small dimensions of the CPM there is no possibility of attaching an SRG sensor directly to the tube body. Therefore, test samples selected for the ultra-sensitive detection of the CPM main seals have to be prepared in two ways. In Fig. 5, two test samples prepared for the ultra-sensitive leak detection of the tube body containing two glass frit seals and of the cathode subassembly sealed to the glass insulation ring with an In alloy are shown. After reduction under an H_2 atmosphere and UHV baking, the tube body is sealed through a graded seal and a glass-to-metal adapter to the test volume consisting of a Vacon 10 (Vacuumschmelze GmbH, Hanau) T-piece, an

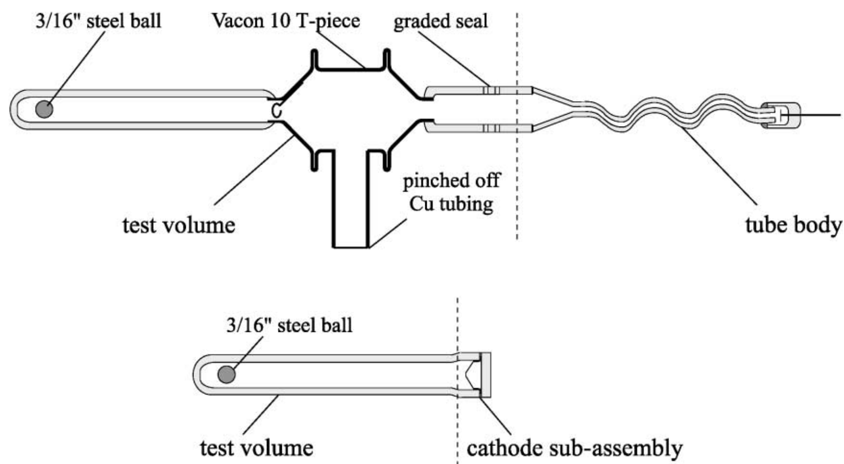

Fig. 5. Test samples prepared for the ultra-sensitive leak detection of the tube body containing two glass frit seals (upper sample) and of the cathode subassembly sealed to the glass insulation ring with In alloy (lower sample).

SRG glass sensor and a Cu tubing. After evacuation and thermal outgassing at 250°C for 10 days, the first test sample is pinched off through Cu cold welding. The second test sample is completed in UHV: the cathode subassembly, without the photocathode and getter, is sealed to the test volume, comprising the glass insulation ring and an SRG thimble made from the same glass, during the course of a vacuum transfer technique.

2.1.2. Permeation of He and accelerated test measurements

Permeation of He through different glass materials is a well-known effect utilized in calibrated test leaks but undesirable in small volume electron tubes such as the new CPMs. Since the permeation of He through the CPM tube body, which consists of different types of soft glass with a high content of PbO, is negligible, we have concentrated on the He permeation through the quartz entrance window.

In order to calculate the equilibrium He flow through a glass wall at a certain He pressure difference, one has to know a permeation constant K. The modelling of a time dependence of an He flow, after a sudden change in He pressure difference, requires the knowledge of the diffusion constant D. The relation between them is given by $K = S \times D$, where S is the solubility of He in the glass.

Available data in literature on the permeation constant K and on the diffusion constant D, both for the He permeation through quartz glass at room temperature (RT), scatter to a large extent [8,9]. Therefore using a He-leak detector, we have made a preliminary measurement of He flow versus time through a quartz faceplate with a thickness $d = 2\,\mathrm{mm}$ and a surface area of about $1\,\mathrm{cm}^2$ after establishing a He pressure difference of 2 bar. From the equilibrium He flow amounting to 5.5×10^{-9} mbarl/s, which is established not before 100 h, we can calculate the RT permeation constant $K \sim 5.5 \times 10^{-10}\,\mathrm{cm}^2/\mathrm{s}$. Numerical integration of the measured He flow as a function of time gives the response time constant $\tau = d^2/6D \sim 50\,\mathrm{h}$ and the corresponding RT diffusion constant $D \sim 3.7 \times 10^{-8}\,\mathrm{cm}^2/\mathrm{s}$.

By numerically solving the diffusion equation we are able to present different examples of the time dependence of He flow through quartz faceplates after a sudden change in He pressure difference, for instance, during the storage of processed CPMs in the air with a partial presure of He of about 5×10^{-3} mbar or after the exposure of CPMs to a higher He pressure for a shorter time. By numeric integration of the He flow in dependence on time we can predict the corresponding He pressure rise versus time in the CPMs.

Using samples similar to the second sample shown in Fig. 5, we can practically observe the He permeation through the quartz faceplate by measuring the He pressure rise versus time, after exposure of the sample to a higher He pressure for a shorter time. Since these samples can be completed during the course of the CPM processing, a getter can be mounted and activated and different photocathode layers can also be deposited, therefore accelerated test measurements of the actual He pressure rise versus time are enabled.

2.2. Internal gases and vacuum transfer technique

Due to the compact design of CPM, the tubes require a radically different vacuum exhaust and process technique than conventional PMTs which could be lined up on a vacuum system manifold and processed individually with the PMT acting as the vacuum chamber. Prototypes of the new CPMs have been processed by a vacuum transfer technique based on the method being used in the fabrication of micro-channel plate (MCP) image intensifiers and photomultipliers. The principles of the vacuum transfer technique are described in two papers on the development of special image tubes for astronomical photon counting applications [10,11]. The major steps of the vacuum transfer technique for the CPM batch processing are schematically presented in Fig. 6 [12]. The new technique consists of UHV baking of the cathode sub-assemblies and the tube bodies, mechanical stirring of the molten In alloy at elevated temperatures, electron (UV light) scrubbing of the tube bodies at RT, photocathode deposition at elevated temperatures, followed by transfer of the

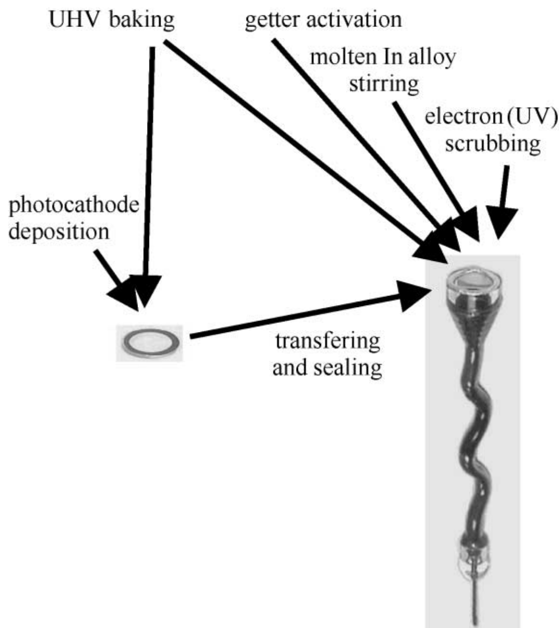

Fig. 6. Major steps of the vacuum transfer technique.

photocathode faceplates to the tube bodies and sealing the CPM components. The separate conditioning of the CPM sub-assemblies including the activation of a non-evaporable getter material, taking place during the UHV baking owing to the low activation temperature, is critical for an extended CPM lifetime.

UHV baking of the CPM sub-assemblies is intended for the thermal outgassing of the cathode sub-assemblies and the tube bodies. After loading a UHV metal chamber, a careful He leak detection of the whole UHV system and start of heating with a slow ramp take place. The thermal outgassing of the CPM components takes place with the loaded UHV chamber heated to the highest temperature (350–400°C) and a high-efficiency sputter-ion pump held at the lowest temperature. In order to thoroughly pump water vapour, the temperature of the sputter-ion pump is, for a shorter time, increased over 100°C. After several hours of thermal outgassing the vacuum system is slowly cooled to RT. The total pressure and partial pressures are continuously monitored using a reliable BAG and a sensitive RGA. At the end of the thermal outgassing phase, the total pressure is of the order of 1×10^{-10} mbar and the residual atmosphere consists mainly of H_2.

Molten In alloy stirring is a very important phase for the correct functioning of the CPM, which has to be performed before the final sealing of the cathode subassembly to the tube body. While cooling down the UHV system, the molten In alloy is mechanically stirred using manipulators, controllable from outside the UHV chamber, in order to thoroughly outgas the applied In alloy. During stirring, the total pressure and partial pressures are controlled using the BAG and the RGA, respectively. The evolving gases which are to be monitored very carefully, supposing that all critical parts involved in the sealing process are prepared in accordance with UHV requirements, are H_2, CO and CH_4.

Electron (UV light) scrubbing of the tube bodies is performed to promote intensive electron and photon stimulated outgassing of the channel walls and the input cone, respectively, as well as for electron gain stabilization. When the loaded UHV chamber is cooled to RT, the electron scrubbing procedure starts. Electron flood guns have been designed to uniformly bombard many tube bodies at once with electrons. The electron scrubbing procedure consists of a low input current/high bias voltage CEM operation and a high input current/ low bias voltage CEM operation, both lasting for a shorter time, and a medium input current/ medium bias voltage CEM operation lasting for a longer time. The input current is related to the output current, which is held constant in all scrubbing modes and approximately equals the maximum linear current (5–10 μA). For a shorter time, UV light is also used to scrub the CEM input cones. During the course of scrubbing, pulse height distribution (PHD), extracted output charge, total pressure and partial pressures, especially those of H_2, CO and CH_4, are monitored. A change in PHD shape and modal gain is related to a change in the channel surface emissive layer composition. The electron gain stability is dependent on the amount of extracted output charge. When ending the scrubbing procedure, the amount of gases remaining in the near surface layer, can decisively influence the CPM operational lifetime.

2.3. Selection and dimensioning of getter material

In field emission displays, MEMS packages and miniature vacuum systems of all kinds with geometry and space constraints, a new generation of high performance, high porosity, thick film getter material (HPTF) has been tested and applied. The new getter, which is deposited on metal strips by SAES Getters' patented screen printing technology, consists of a mixture of Ti and Zr–V–Fe alloy. The high porosity of 60–65% corresponds to a ratio of active surface area over a geometrical one amounting to 20–30 for typical 100 μm coatings. The total sorption capacity for CO is of about 7×10^{-4} mbarl/cm^2 and that for H_2 is more than 1×10^{-2} mbarl/cm^2. The temperature of getter activation lies in the range from 300–500°C, therefore the activation takes place during the UHV baking phase.

The selection of a proper getter material is decisive for the extended CPM lifetime. Therefore, the use of the high performance HPTF getter has also been foreseen for a new CPM. Incorporating the selected getter, the CPM becomes actually a miniature static vacuum system with a small volume ($V \sim 0.3$ cm^3) and a relatively large inner surface area ($S \sim 4$ cm^2) evolving gases with different outgassing rates. In fact, getter dimensioning depends on the space available for its mounting and on the estimated gas load.

For calulating the amount of getter material necessary to capture the gas released during device storing and operation, data on outgassing rate versus time are needed. It is customary to assume a time dependence of the CO outgassing rate $q \propto t^{-1}$, used for gases, which are desorbed from the surface of a material, and a time dependence of the H_2 outgassing rate $q \propto t^{-1/2}$, used for gases which desorb by diffusion from the bulk of a material. The resulting gas load $V\,\Delta P$ is proportional to ln t and $t^{1/2}$, respectively, where ΔP is the increase in pressure inside the volume V with no getter mounted. After expiration of a certain time, the gas load in the first case is considerably lower. Nevertheless, it is customary to overdimension the amount of getter material by considering a safe time dependence of the H_2 outgassing rate and a safe total sorption capacity for CO for all gases released. The HPTF getter with a geometric surface area of 0.1 cm^2, dimensioned in accordance with the CPM space available for its mounting, is therefore believed to cope with RT outgassing with an initial rate of 1×10^{-9} mbarl/s cm^2 for about 2 years, when the total gas load amounts to 6.3×10^{-5} mbarl, and with RT outgassing with an initial outgassing rate of 1×10^{-10} mbarl/scm^2, for about 200 years, until the same total gas load is reached.

According to the engineering calculation above, a mild UHV baking is sufficient to reduce the RT initial outgassing rate below 1×10^{-10} mbarl/s cm^2 and a modest electron scrubbing can be performed to reduce the electron stimulated outgassing rate to below the low 10^{-10} mbarl/s cm^2 range. But we are convinced that this scenario is not possible. Experiences with SRG measurements of pressure rise versus time performed at RT in baked and sealed off UHV metal chambers, in which the outgassing of H_2 with a constant outgassing rate (with no re-adsorption of H_2) takes place [13], indicate that we have to consider a constant RT outgassing rate of H_2 $q = q_0$ inside our miniature electron tube. In this case the gas load is linearly dependent on time: $V\,\Delta P = Sq_0\,t$. Choosing the same amount of HPTF getter with a total sorption capacity for H_2 of 1×10^{-3} mbarl, the getter is able to cope with RT outgassing at a constant outgassing rate of 1×10^{-12} mbarl/s cm^2 for about 8 years.

In addition, when using a bulk Zr–Ti–Ni getter to pump H_2 in the presence of small quantities of CO, with their molar ratio in the range between 3 and 30, the pumping speed for H_2 falls rapidly after consuming less than 5% of the total getter sorption capacity for H_2 [14]. This result has been seriously considered, since a CO passivation layer of the order of monolayer dimensions may affect the RT sorption process of H_2, consisting of adsorption of H_2 molecules, surface dissociation and diffusion of H atoms into the bulk getter. On the other hand, the degree of getter activation depends on the temperature applied during the UHV baking and on the UHV baking time. According to the producer's data, the effect of activation at 360°C for 10 h is of about 90% compared to that of full activation. Once activated

the getter starts to act as an in-situ pump, therefore it is necessary to consider the amount of getter material consumed during the course of the CPM processing until the final sealing is done. If an average working pressure of 1×10^{-8} mbar, due to outgassing of alkali dispensers during hypothetical photocathode activation, which takes place at elevated temperatures for 3 h, and a getter pumping speed of 0.1 l/s is assumed, then about 15% of the total sorption capacity for CO is consumed.

According to the new calculation and considering the additional effects and circumstances, a thorough UHV baking is needed to reduce the RT outgassing rate to 1×10^{-14} mbarl/s cm^2 and even below, and a sufficient electron scrubbing has to be performed while operating CEMs in the medium input current/medium bias voltage scrubbing mode to reduce the electron stimulated outgassing rate below 1×10^{-11} mbarl/s cm^2. If the CEM active surface area equals about a half of the CPM inner surface area, then an operational CPM lifetime in excess of 10 years is estimated.

3. Results

After bake-out and pinch-off of the first test sample shown in Fig. 5, the ultra-sensitive leak detection of the tube body with two glass frit seals was performed. In Fig. 7, measurement of pressure rise versus time inside this sample with a volume of about 24 cm^3 is shown. An SRG thimble is made from a kovar glass tubing in order to reduce the effect of metal housing tubes on the zero stability of SRGs [15]. From the pressure rise behaviour one can see the influence of temperature variations inside a ± 1°C range. Deviations from a linear increase are due to the effect of ambient temperature on the offset correction of SRGs [16]. The slope of the linear part of the pressure rise curve inside the 15 day time interval gives a total outgassing rate of 7.4×10^{-15} mbarl/s (N_2 equivalent). If considering an estimated RT permeation constant for the He permeation through a kovar glass of 5.3×10^{-12} cm^2/s, the estimated He flow rate due to permeation of atmospheric He through the kovar glass tubing with a thickness of 0.85 mm

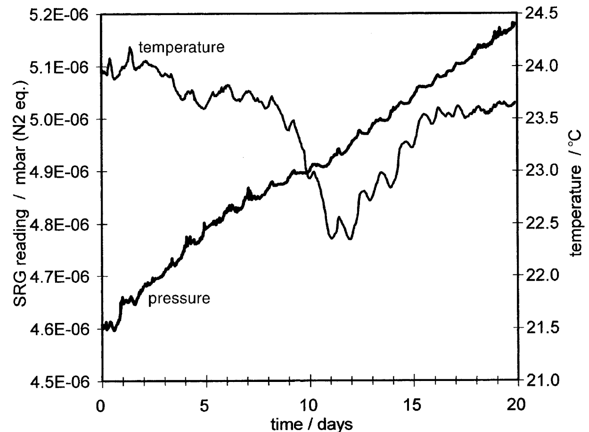

Fig. 7. Pressure rise versus time, inside the test sample with a volume of about of 24 cm^3, measured at RT using an SRG.

and a surface area of 15.3 cm^2 amounts to about 1.8×10^{-15} mbarl/s (N_2 equivalent). We assume that the difference between the total outgassing rate and the He permeation flow rate of 5.6×10^{-15} mbarl/s can be due to H_2 evolving from metal parts corresponding to an estimate of H_2 RT outgassing rate of about 1×10^{-15} mbarl/s cm^2.

About one month after processing and transportation of the second test sample shown in Fig. 5, the ultra-sensitive leak-detection of the cathode subassembly sealed to the glass insulation ring with an In alloy was performed. The ambient temperature is adjusted inside a ± 0.1°C range. A linear dependence of pressure rise versus time is measured on the test sample with a volume of about 1.5 cm^3 giving a total outgassing rate of about 3.5×10^{-15} mbarl/s (He equivalent). The calculated He flow rate due to atmospheric He permeation through a quartz input window with a thickness of 2 mm and a surface area of 0.3 cm^2 amounts to 3.8×10^{-15} mbarl/s indicating that the measured test sample is extremely vacuum tight.

Results of the modelling of the rate of He pressure rise inside the CPM with a volume of 0.3 cm^3 due to atmospheric He permeation through the quartz input window and due to the He permeation through the same window after exposure of the CPM to 1 bar of He for 1 h, are

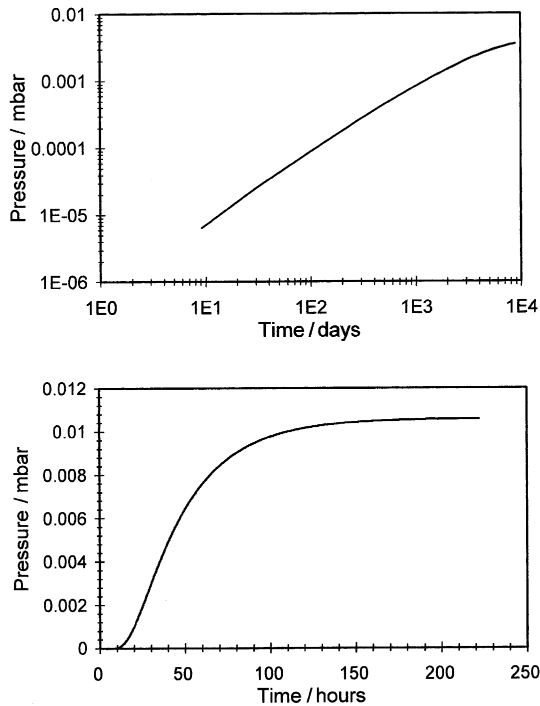

Fig. 8. Results of the modelling of a rate of He pressure rise inside the CPM due to the atmospheric He permeation through the quartz input window of a thickness of 2 mm and a surface area of $0.3\,cm^2$ (upper diagram) and due to He permeation through the same quartz faceplate after exposure of the CPM to 1 bar of He for 1 h (lower diagram).

presented in Fig. 8. The first diagram shows that a He pressure rise to 1×10^{-3} mbar is reached in about 3 years. At pressures of this order of magnitude, bombardment of the photocathode surface with He ions does not result in photocathode surface sputtering but in ejection of additional electrons due to the secondary emission effect. When CPMs operate in the photon counting mode after-pulses, which follow the main pulse, are a consequence of this effect. The second diagram shows that a He pressure rise in excess of 1×10^{-2} mbar is reached in about 5 days. On approaching this pressure range arcing at the channel exit starts followed by CPM breakdown, an event which is proved experimentally.

The molten In alloy stirring is performed before the final sealing of the cathode sub-assembly to the tube body. This phase is performed, using wobble-stick manipulators, towards the end of the UHV baking phase while cooling down the UHV system. During the stirring, total pressure and partial pressures are monitored. Normally, the intensity of evolving gases decreases strongly from H_2 to CO and finally to CH_4. This was not the case for some time in the early stages of CPM development when looking for the most suitable vacuum deposition technique of metallization layers. Using the metal soldering technique the metallization layers are needed to achieve a reliable and vacuum-tight sealing of the glass parts. The upper diagram in Fig. 9 surprisingly shows, besides the outgassing of the mentioned gases, a relatively high outgassing of Ar during the molten In alloy stirring performed just before the final sealing phase. Ar outgassing of almost the same intensity continues during the sealing procedure which follows. The sealing procedure was even repeated three times, starting with a simultaneous lifting of the photocathode faceplates, but with no essential reduction in the outgassing of Ar. All six processed CPM samples did not survive the first operational test because of a strong glow forming at the channel exit (the bias voltage amounted to about 1500 V only) resulting in tube breakdown. The lower diagram in Fig. 9 shows the gas composition during the molten In alloy stirring of three samples with the metallization layers deposited by sputtering in an Ar atmosphere and three samples with the metallization layers deposited by vacuum evaporation. The difference concerning the outgassing of Ar is obvious. With this trial it has been proven that the sputtered metallization layers are not usable at all for the metal soldering technique, since the Ar incorporated to a large extent in the sputtered layers is, after their wetting, dissolved in great quantities in the molten In alloy. In addition, UHV pre-baking of tube bodies with the sputtered metallization layers at 350°C for 5 h did not bring any noticeable improvement concerning the harmful Ar outgassing effect.

Excluding the defect described above the electron and UV light scrubbing of the tube bodies, intended for the intensive electron and photon stimulated outgassing of the channel walls and the input cone, respectively, are the most decisive phases for an extended CPM operational lifetime.

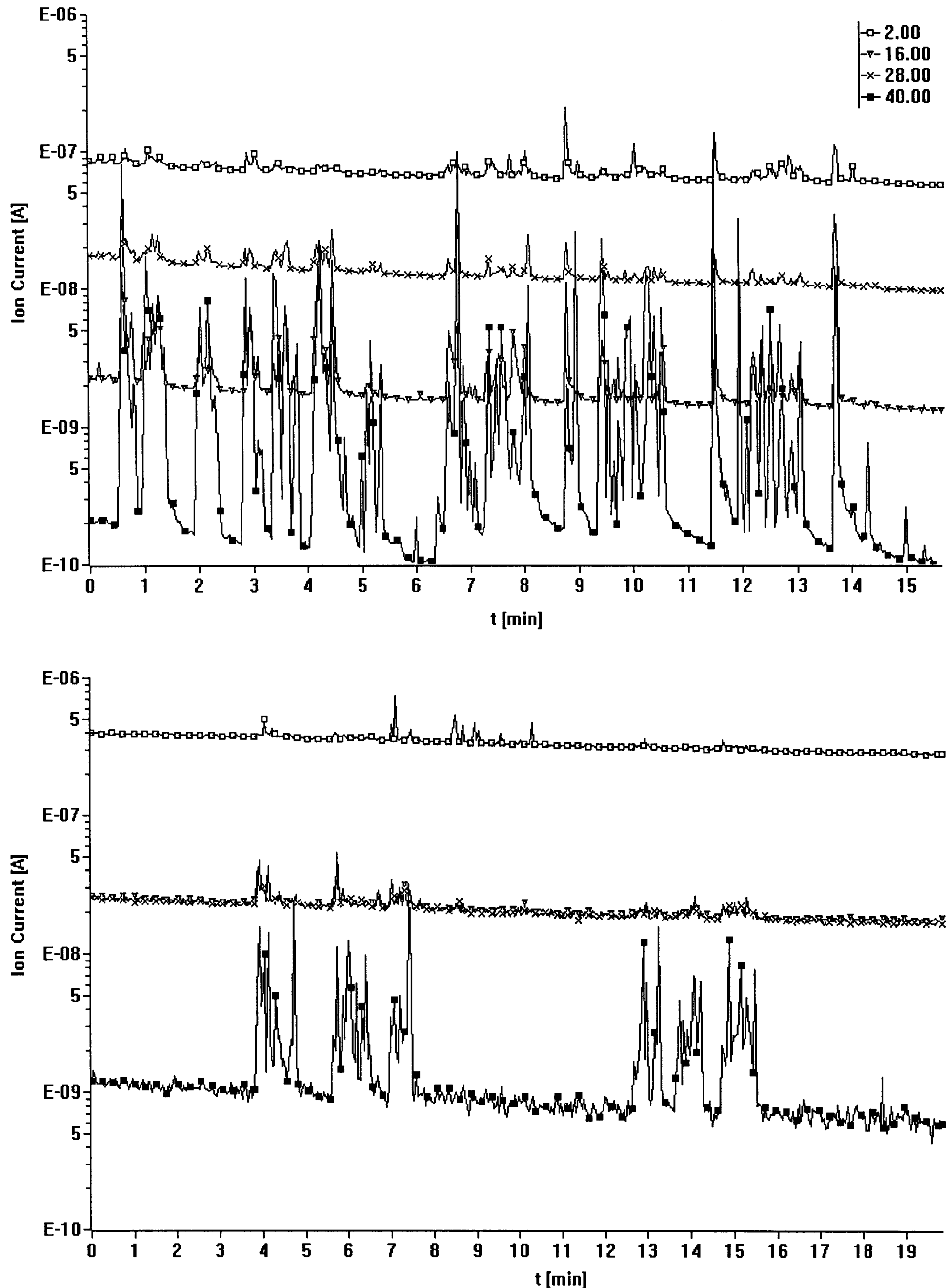

Fig. 9. Outgassing of Ar, at $T = 92°C$ and $P = 1.5 \times 10^{-9}$ mbar, during the molten In alloy stirring (recorded from 0.5 to 5.5 min) and during the sealing of the photocathode faceplates to the tube bodies (recorded from 6.5 to 8.5 min); the sealing is repeated three times starting with a simultaneous lifting of the faceplates at 9, 11.5 and 14 min (upper diagram); gas composition during the alternating molten In alloy stirring at $T = 140°C$ and $P = 5.5 \times 10^{-9}$ mbar of three samples with metallization layers deposited by sputtering in Ar atmosphere (recorded from 3.5 to 7.5 min and from 12.5 to 15.5 min) and three samples with metallization layers deposited by vacuum evaporation (recorded from 8.5 to 10.5 min and from 16.5 to 19.5 min) (lower diagram).

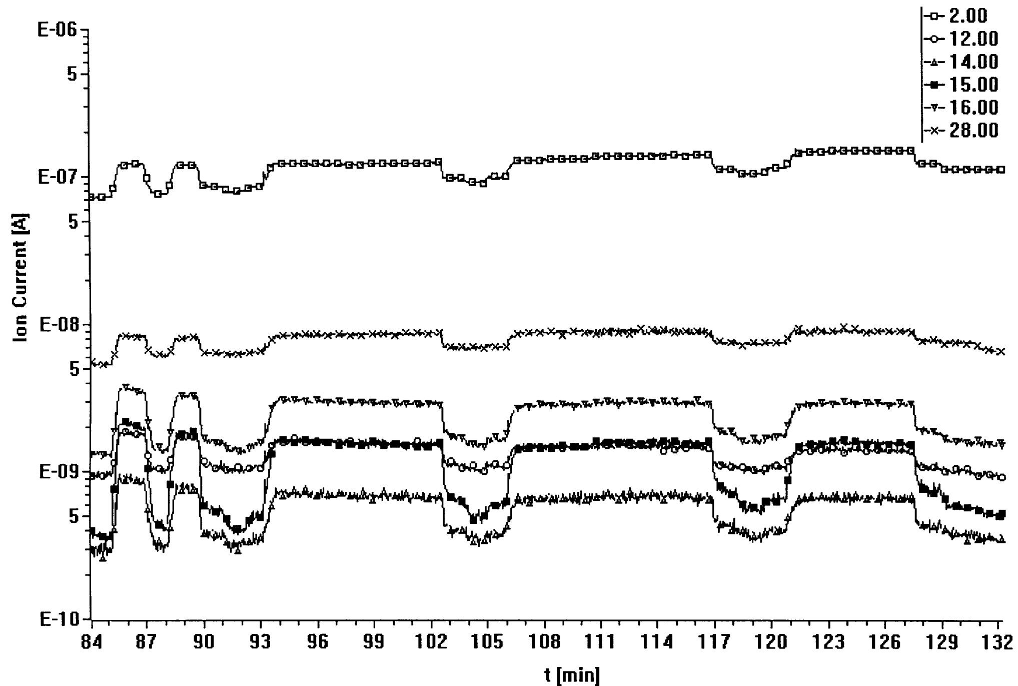

Fig. 10. Outgassing of H_2, CO and CH_4 during electron scrubbing of CEMs operating in a high input current/low bias voltage mode at RT and a residual pressure of 1×10^{-10} mbar; the electron scrubbing is interrupted for a few periods by switching off the bias voltage at 90, 102, 116,5 and 127 min, and the electron gun screen voltage at 86, 91, 103.5, 118 and 129 min in alternation with switching on the bias voltage at 93, 106 and 120.5 min, and the electron gun screen voltage at 88, 92, 104,5 and 119.5 min, concluding by switching off the electron gun filament current at 131 min, in order to eliminate the outgassing due to the CEMs operation from other effects.

The electron flood gun has been constructed to uniformly bombard a larger group of tube bodies with electrons. The electron scrubbing takes place at RT and a total pressure of about 1×10^{-10} mbar. Depending on the scrubbing regime applied, the tube bodies can be heated even in excess of 100°C by the channel resistive heating. In Fig. 10, the main outgassing components recorded during the course of the electron scrubbing of the tube bodies, operating in a high input current/low bias voltage scrubbing mode are shown. Choosing a bias voltage of 1200 V the output current is adjusted between 5 and 10 μA by raising the heating current of the electron flood gun filament. Using this scrubbing regime the outgassing is very effective, since the channel walls are bombarded with electrons along the whole channel. The principal evolving gas species is hydrogen, followed, in descending order, by carbon monoxide and methane. The partial pressure of H_2, which is outgassed from the channel near the surface conductive layer, is by more than one order of magnitude higher than those of CO and CH_4. Any chemisorbed water, resulted from the reduction of the tube bodies under H_2 atmosphere and their exposure to the atmosphere, which remains after the UHV baking is dissociated under electron bombardment, yielding H_2 and O. The atomic oxygen quickly reacts with the carbon present in the whole system to form CO and to a lesser extent CO_2, therefore the amount of both gases produced in the tube bodies is unknown. Dissociation of any hydrocarbons present produces CH_4 [10]. The characteristic mass to follow methane is mass 15, since it represents 85% of the main methane mass 16, which is otherwise difficult to resolve from contributions of other gases. The electron scrubbing is interrupted for some periods by consecutive switching off the bias voltage and the electron gun screen voltage

followed by consecutively switching on in the opposite order, and at its conclusion by switching off the electron gun filament current, in order to eliminate outgassing due to the CEMs operation from other effects. During the high input current/low bias voltage scrubbing phase (lasting for about 45 min), the change in total pressure due to the channel outgassing decreases from 1.5×10^{-10} to 6×10^{-11} mbar. It must be stressed that the described scrubbing process is pretty severe, being rarely used in most CPM applications.

4. Discussion

The CEMs incorporated in the new CPMs are designed in the form of a serpentine to prevent a phenomenon known as ion feedback. Due to the high electron densities, existing within the channel near the output end, gases adsorbed on the surface of the walls are desorbed and ionized, forming positive ions (see Fig. 2). In the case of a straight channel, these ions travel back towards the channel input and proceed to the photocathode. When they strike the channel input walls or the photocathode surface and, with a kinetic energy of the order of kilovolts, they produce secondary electrons which are subsequently amplified and detected at the output end as a spurious pulse, following the main pulse. This noise pulse is therefore called an after-pulse. Electron gains in excess of about 10^4–10^5 cannot be sustained in straight channel geometry devices [4]. Curving the channel effectively reduces this problem by preventing gas ions from travelling far enough to gain sufficient energy to produce secondary electrons on their way towards the channel input. In this case, the photocathode surface is bombarded by gas ions with a kinetic energy of the order of a hundred volts due to ionization of gas molecules leaving the channel or desorbing from the input cone. However, due to the curved channel the CPMs can achieve analogue electron gains of 10^7 or more and photon counting electron gains in excess of 10^8.

Where exceeding electron gain values of 10^8, a saturation effect, due to space charge build-up near the output end of the channel occurs. When

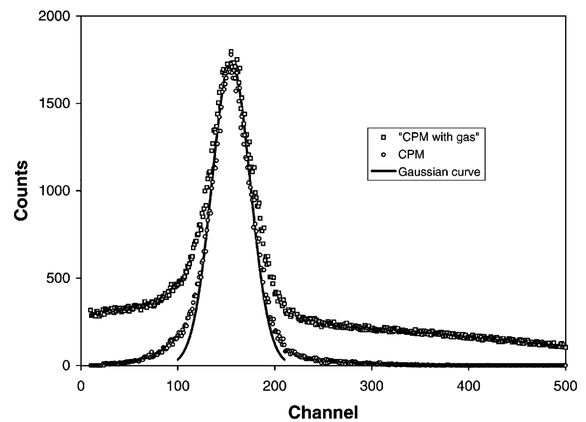

Fig. 11. Pulse height distribution (PHD) of single photoelectron events, taken from a typical CPM by a multi channel analyser: the PHD is nearly of the Gaussian shape exhibiting a high modal gain, a very narrow resolution, and especially a very high peak to valley ratio due to the absence of 'dynode noise'; for comparison a PHD with a similar modal gain of a CPM sample classified as a 'CPM with gas' is added: a higher valley level on the left-hand side of the PHD is assumed to be due to local non-uniformity of the mean secondary emission coefficient in the channel, but a tail on the right-hand side of the PHD, extended towards the higher electron gains, is due to the increased pressure and intensive ion bombardment of the photocathode surface resulting in the ejection of secondary electrons and formation of after-pulses.

CPMs operate in a photon counting or saturation mode, the output pulses are nearly of constant amplitude. In Fig. 11, a pulse height distribution (PHD) of single photoelectron events, taken by a multi channel analyser is presented. The PHD is nearly of Gaussian shape exhibiting a high modal gain, which is a function of the secondary emission coefficient of the glass, the applied voltage and the length-to-diameter ratio of the channel, a very narrow resolution due to a small statistical spread in the secondary emission coefficient around the mean value, and especially a very high peak-to-valley ratio due to the absence of the 'dynode noise' being typical for conventional PMTs. In the same diagram, a PHD with a similar modal gain of a CPM sample classified and rejected as a 'CPM with gas' is shown, meaning that the pressure inside such a sample has increased. The valley on the left-hand side of the PHD is raised to a higher level and the tail on the right-hand side of the

PHD is extended towards the higher electron gains, due to the increased number of fractional and multi-photoelectron pulses, respectively, if supposing that a peak of the PHD corresponds to one photoelectron equivalent. Following experience with hundreds of PHD measurements, we can attribute the right tail to the increased pressure and the intensive ion bombardment of the photocathode surface, resulting in the ejection of secondary electrons and formation of spurious pulses known as after-pulses. The production of secondary electrons by potential ejection is very effective due to the big difference between the excitation energy (ionization potential) of gas ions ranging from 12 to 25 eV and twice the work function of semiconductive photocathodes ranging from 1.3 to 2 eV. Since the incorporated CEMs are extremely 'silent' we assume that a lower peak-to-valley ratio is due to local non-uniformity of the mean secondary emission coefficient in the channel. Spurious pulses due to the ion bombardment of the channel walls and the production of secondary electrons by potential ejection are less probable, except in the case of the bombardment with He ions, since the estimated work function of the channel surface emissive layer amounts to between 7.3 and 9.7 eV [4]. It has been confirmed by measurements that an increased valley level may also appear with CPMs which show no signs of 'bad vacuum'.

In addition, all conventional PMTs exhibit, besides a relatively high dynode noise, the phenomenon of after-pulses, where a proportion of signal pulses is followed by time correlated spurious pulses with electron gains ranging from a fraction of a photoelectron equivalent up to 10 photoelectron equivalents [17]. Fractional photoelectron pulses with conventional PMTs, due to the ion bombardment of dynodes and the production of secondary electrons by potential ejection are more probable, since the work function of the applied metal dynodes is considerably lower than that of the channel surface emissive layer. Since the multi-photoelectron pulses contribute to dark counts in proportion to their number and to anode dark current in proportion to their number and pulse height [17], the measurement error, while using the CPMs operating either in photon counting or direct current mode, is greatly reduced by maintaining UHV conditions in order to avoid the formation of after-pulses.

5. Conclusion

The extended CPM lifetime depends on the amount of gas load, which can be accumulated inside the CPM, during storage and operation, and can be at the same time sorbed by the incorporated getter. The gas load, resulting from metal solder outgassing during the CPM final sealing, ambient temperature outgassing of the CPM inner surfaces and electron (photon) stimulated outgassing from CEMs including ultra-fine leaks through the main CPM seals, has been reduced to a great extent. The getter activation is performed following a temperature schedule of the UHV baking phase and the getter consumption has been minimized due to the optimized UHV conditioning of the tube parts. All improvements have been enabled due to the meticulous preparation of the CPM subassemblies and other auxiliary parts, and due to the maintenance of extreme vacuum conditions during the course of the vacuum transfer technique.

Inert gases are not sorbed at all by any getter material. Therefore, any penetration of Ar, Ne and He from air atmosphere and accumulation of these gases inside the CPMs must be prevented. Extreme vacuum tightness of the main CPM seals is tested by sampling and applying an ultra-sensitive leak detection method. He permeation through quartz faceplates can only be prevented by storing the corresponding CPMs under a protective atmosphere.

Since firing in hydrogen is the last phase of the tube body preparation a certain quantity of hydrogen is dissolved in the conductive channel surface layer to a thickness of a few hundreds of nanometres[4], therefore, hydrogen is the most potential gas to evolve. Although the hydrogen outgassing is unavoidable, it can be reduced by a thorough UHV thermal treatment and an effective electron scrubbing procedure. The incorporation of a high performance getter with an enlarged total sorption capacity for hydrogen should guarantee an extended CPM lifetime.

Production of carbon monoxide from reactions of system water with carbon on hot filaments and from electron induced dissociation of chemisorbed water, resulted from hydrogen firing of the channel glass walls and exposure of the channel surface layer to the atmosphere, which remains after the UHV baking, can only be reduced by a thorough thermal outgassing of the loaded UHV chamber. Controlling this important phase a premature poisoning of the getter surface with carbon monoxide which may affect the hydrogen pumping speed is prevented. Regarding the glass material, the maximum UHV baking temperature should be in excess of 385°C in order to overcome the 'second water peak', well-known from the production of MCP image intensifiers, which appears when raising the baking temperature over 350°C.

Methane produced from the cracking of hydrocarbons eventually present in the CPMs is not sorbed at RT by the incorporated getter material therefore the methane partial pressure is to be carefully observed during the vacuum deposition of the metallization layers, vacuum firing of the auxiliary parts and UHV baking of the UHV chamber loaded with the tube sub-assemblies. In order to fully minimize the contamination with hydrocarbons all production vacuum systems are equipped with dry vacuum pumps.

Acknowledgements

The channel photomultiplier has been developed and introduced into the pilot production at Heimann Opto, PerkinElmer Optoelectronics in Wiesbaden, Germany. The author would like to thank R. Barden and A. Hatzenbühler, both from Heimann Opto, for their help in performing measurements in Wiesbaden, and J. Šetina from Institute of Metals and Technology in Ljubljana, Slovenia for his precise realization of SRG measurements.

References

[1] Barden R, Erjavec B. Vakuumist 1999;19:4 (in Slovene).
[2] Barden R. Photonik 2000;1:32.
[3] Barden R. Elektronik 2000;9:90.
[4] CHANNELTRON® Electron Multiplier, Handbook for Mass Spectrometry Applications, GALILEO Electro-optics Corp., 1991.
[5] Erjavec B. Thin Solid Films 1997;303:4.
[6] Jenko M, Erjavec B, Praèek B. Vacuum 1990;40:77.
[7] Šetina J, Zavašnik R, Nemaniè V. J Vac Sci Technol 1987;A5:2650.
[8] Readhed PA, Hobson JP, Kornelsen EV. The physical basis of ultrahigh vacuum. Woodbury, NY: AIP Press, 1993.
[9] Roth A. Vacuum technology. Amsterdam, New York, Oxford: North-Holland:, 1982.
[10] Norton TJ, Airey RW, Morgan BL, Read PD, Powell JR. Adv EEP 1988;74:41.
[11] Beaver EA, Acton L, Doliber D, Dozier E, Wenzel H. Adv EEP 1988;74:347.
[12] Erjavec B. Mater Technol 2000;34:437 (in Slovene).
[13] Berman A, Fremerey JK. J Vac Sci Technol 1987;A5:2436.
[14] Mehshoff TK, Barnes LW. J Vac Sci Technol 1984;A2:1213.
[15] Šetina J. Vacuum 1990;41:2115.
[16] Šetina J. Vacuum 1990;40:51.
[17] Wright AG. Nucl Instr Methods A 1999;433:507.